NASA TN D-1055

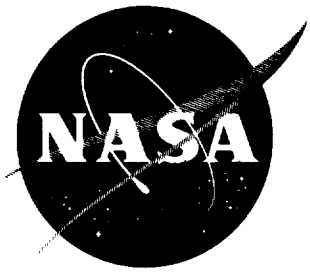

TECHNICAL NOTE
D-1055

THE NEUTRALIZATION OF ION-ROCKET BEAMS

By Harold R. Kaufman

Lewis Research Center
Cleveland, Ohio

NATIONAL AERONAUTICS AND SPACE ADMINISTRATION
WASHINGTON

August 1961

M

NATIONAL AERONAUTICS AND SPACE ADMINISTRATION

TECHNICAL NOTE D-1055

THE NEUTRALIZATION OF ION-ROCKET BEAMS

By Harold R. Kaufman

SUMMARY

The experimental ion-beam behavior obtained without neutralizers is compared with both simple collision theory and plasma-wave theory. This comparison indicates that plasma waves play an important part in beam behavior, although the present state of plasma-wave theory does not permit more than a qualitative comparison. The theories of immersed-emitter and electron-trap neutralizer operation are discussed; and, to the extent permitted by experimental data, the theory is compared with experimental results. Experimental data are lacking completely at the present time for operation in space. The results that might be expected in space and the means of simulating such operation in Earth-bound facilities, however, are discussed.

INTRODUCTION

What happens downstream of an ion rocket is not important as long as the engine continues to operate and produce thrust. There is, however, a distinct possibility that phenomena occurring behind an ion rocket in space will reduce its thrust or even stop its operation completely. This possibility provides the motivation for study in the neutralization area.

As mentioned in reference 1, the need for neutralization is twofold. First, the ejection of electrons and ions should be at equal rates to avoid a buildup of charge on the space vehicle. If the ejection rates are equal, then current neutralization is obtained. Second, the electrons must be added in such a way that the charge density of the beam is neutral, to avoid beam turnaround. This condition of equal electron and ion densities, giving zero net charge density in the beam, is called "charge neutralization."

The space vehicle potential changes so rapidly when current neutralization is not obtained that the ion-accelerator operation can be

stopped in microseconds. The space vehicle potential could be measured, and an electronic control could conceivably regulate the neutralizer electron current in a sufficiently rapid fashion to avoid buildup of space vehicle potential. A far more practical solution, though, is to make the neutralizer self-regulating. That is, an increase (positive) in space vehicle potential should decrease the rate of electron ejection from the neutralizer, while a decrease of space vehicle potential should increase this rate. Such a self-regulating behavior can be obtained by having the flow of electrons from the emitter to the ion beam be space-charge-limited rather than emission-limited. Thus, the space vehicle potential is felt at the electron emitter, and the potential difference between the emitter and the beam might be expected to adjust and give the desired electron current. Whether or not such self-regulation does in fact occur is part of the subject matter of this report.

Charge neutralization of the ion beam is made difficult by the small mass of electrons. For much of the specific-impulse range of interest, just the thermal energy from the hot emitter is sufficient to give the electrons a mean velocity exceeding that of the ions. To minimize this velocity problem, a neutralizer should obviously operate with a minimum potential difference between the emitter and the beam.

Various neutralizer configurations have been proposed, but the designs that have had some degree of success to date fall into two general categories. The simplest is the immersed-emitter type (refs. 2 and 3) in which an electron emitter is placed in the beam. A virtual anode forms at about the distance from the electron emitter where the emitted electron density equals the ion density. The acceleration distance for the electrons with space-charge-limited flow can thus be a small fraction of a millimeter, permitting very small accelerating potential differences to be used. The immersed-emitter type suffers the disadvantage of sputtering erosion. Careful design, however, can keep the erosion rate well under 1 percent of propellant flow rate.

The other general category of neutralizer is the electron-trap type (refs. 4 and 5) in which the electron-emitter surrounds, but is not in, the beam. The positive ions in the beam produce a potential difference sufficient to draw the required electrons from the emitter to the beam. The portion of the beam enclosed in the neutralizer structure is assumed to be positive relative to the remainder of the beam. The potential difference between the emitter and the portion of the beam in the neutralizer can, therefore, be considerably larger than the net difference between the emitter and the beam outside of the neutralizer. The electron-trap neutralizer can thus be said to employ accel-decel to reduce electron velocity in the beam.

The beam mechanisms involved in the operation of these neutralization devices have not been adequately explained. Hence, the effectiveness of these neutralizers in space is in doubt. This report is an

order-of-magnitude study of beam phenomena - comparing experiment and theory. The object of this study is, of course, to throw some light on the problem of neutralization in space. The state of the art of neutralization being what it is, the results of the study are largely speculative in nature.

Most experimental data in test facilities have been obtained in operation without neutralizers; thus, such operation is a convenient starting point for the study. The operation without neutralizers is compared first with simple collision theory. Then the operation is compared with plasma-wave theory. Next, the operation in test facilities with neutralizers is examined. Finally, although experimental data are lacking, operation with neutralizers in space is considered.

Various sources were used for experimental data, as indicated by the references. Unfortunately, it is beyond the scope of this report to give credit to all those who have contributed to the areas discussed. Further, the author is most familiar with work done at the Lewis Research Center, which leads to a natural preponderance of such data.

OPERATION WITHOUT NEUTRALIZERS IN TEST FACILITIES

At first glance, an ion rocket might not be expected to operate in a test facility if a neutralizer is not used. In practice, however, ion rockets do operate under such conditions, although that operation often leaves much to be desired. The explanation is that current neutralization is not needed because the ion engine is usually electrically connected to the target, while electrons from the target and the residual gas provide charge neutralization. Indeed, the problem in many experiments is to keep the electrons out of the beam, rather than in it.

Most ion-rocket experiments at the Lewis Research Center have been conducted in the 5-foot-diameter, 16-foot-long vacuum tanks described in reference 6. The typical ion-beam currents have ranged from 10 to several hundred milliamperes, while the ion energies have ranged from about 1000 to 20,000 electron volts (ev).

Observation of many of these experiments at Lewis indicates that operating characteristics can be classified by neutral density. High-neutral-density operation at or above an ion-gage reading of 10^{-5} millimeters of mercury (mm Hg) has generally been stable as far as overall beam measurements are concerned. Readings slightly above 10^{-5} mm Hg have been required to make the beam visible, while readings substantially above 10^{-5} are associated with electrical breakdown and therefore are not used for engine operation.

Low-neutral-density operation, at or below readings of 10^{-6} mm Hg, has been typically accompanied by random sparks wherever the beam came near a conducting surface. As described in reference 7, these sparks introduced undesirable transients to the engine by way of the beam, which is a conducting plasma.

Between ion-gage readings of 10^{-5} and 10^{-6} mm Hg the operation changes, of course, from one mode to the other. The exact pressure at which this change occurs apparently depends on such parameters as specific impulse, beam current, beam length, and type of ion.

Another form of sparking, which can be confused with the beam sparking observed at low neutral densities, was found. Charge exchange and ionization processes produce low-velocity ions. These ions move radially outward from the beam and, with a few stray electrons, can fill the test chamber with a dilute plasma. At high neutral densities and ion-beam currents, where the production rate of low-velocity ions is high, sparks are often observed in regions far from the beam. Electrical breakdown at the engine can be frequent unless the engine is screened from this plasma. Sparks of this nature will be ignored in this analysis.

It should be mentioned that the ion-gage readings were not corrected for the type of molecule in the test facility and hence would be correct only if the residual gas was predominantly air. The uncorrected readings vary as the product of ionization cross section and neutral density $\partial_i n_o$, while the corrected values vary only as the neutral density n_o. The effect of neutrals on ion-beam behavior is through collision processes and hence would vary as the product of some collision cross section and the neutral density ∂n_o. Since the various cross sections are roughly proportional for different atoms, the uncorrected reading is probably more significant for ion-rocket operation than the corrected value.

Collision Processes

The phenomena included in collision processes are secondary emission from ion bombardment of surfaces; elastic, exciting, and ionizing two-body collisions; and soft or coulomb collisions between charged particles. A first attempt to explain observed ion-beam behavior was made using these collision processes. Although the collision-process approach does not by itself adequately explain observed phenomena, it is useful as a foundation for more complete theories.

The conditions assumed for these processes were a mercury-ion-beam density of 10^9 per cubic centimeter, moving at a velocity of 4.9×10^6 centimeters per second (corresponding to a specific impulse of 5000 sec) over a beam length of 1 meter. The neutral gas was assumed to be mercury at a density of 10^{10} for an ion-gage reading of 10^{-6} mm Hg, and 10^{11} for

an ion-gage reading of 10^{-5} mm Hg. About the only effect of the use of an element other than mercury would be to shift the thresholds for excitation and ionization a few ev. The conclusions drawn would be substantially the same. The sources for the collision-process data and the assumptions involved are presented in the appendix.

The normal condition for an ion beam in a test facility is substantially charge-neutralized. Because the electrons are usually moving at many times ion velocity, they tend to escape to conductors in contact with the beam, leaving the beam with a net positive charge and a positive potential relative to those conductors. The beam potential reached will still be much smaller than that which would be obtained if all the electrons were suddenly removed. The gross ratio of electrons to ions throughout the beam is, therefore, approximately unity. Thus, the electron density in the ion beam was also assumed to be about 10^9 per cubic centimeter throughout the analysis.

The beam dimensions are many times the Debye shielding distance, so the net beam charge resides almost entirely near the physical limits of the beam. The resultant potential variation is shown in sketch (a):

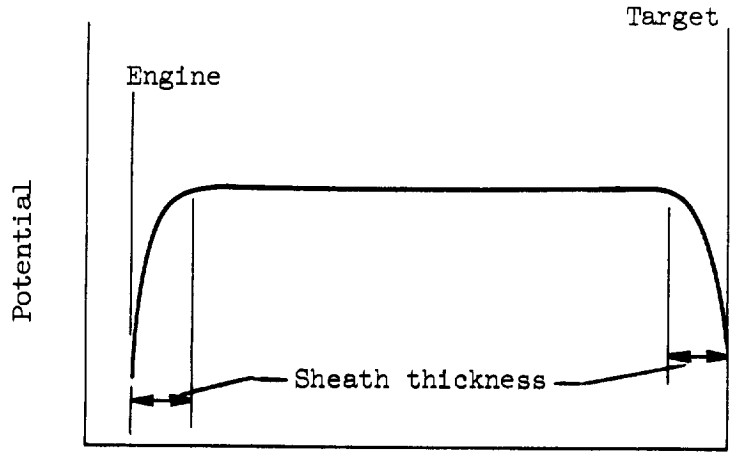

(a)

Almost all the potential variation is limited to the sheaths that form at the ends and sides of the beam. These sheaths would be of the order of 1 to several millimeters thick for an electron temperature of 10 ev and the conditions assumed previously. The depth of the potential well for electrons in sketch (a) is presumably determined by the collision processes that add electrons to, and remove electrons from, the beam. The

equilibrium depth is obtained when the rate of electron addition to the beam is just balanced by the electron losses from the beam. This discussion of sheath phenomena is a much simplified picture that will be modified as the analysis progresses.

The electron temperature enters into almost any plasma calculation, so the determination of equilibrium temperature from collision processes is of interest. The equilibrium electron temperature will be calculated first for the condition of no electron gains or losses to provide an introduction to the more complicated case that would actually be expected. The characteristic times for electron-energy gain or loss are shown in sketch (b) as a function of electron energy:

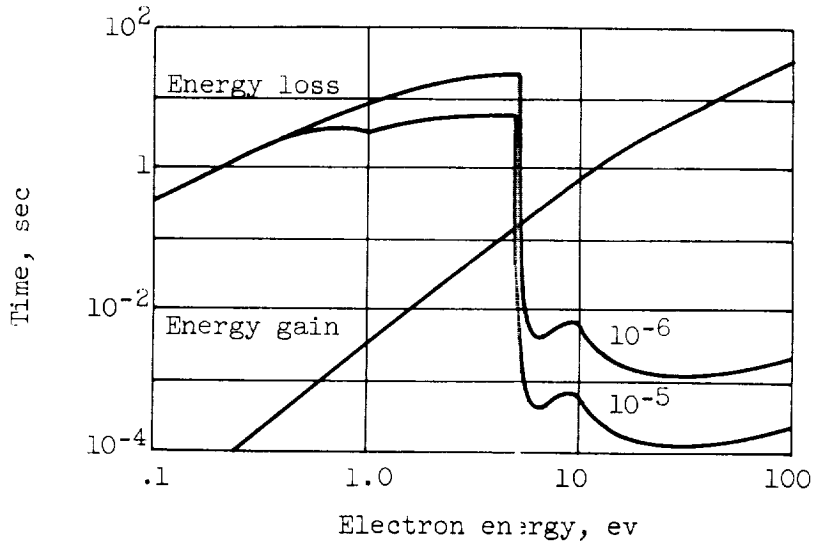

(b)

Collision processes can be shown in terms of various parameters such as cross sections, mean path lengths, secondary emission coefficients, or characteristic times. It was felt that all processes should be presented in terms of the same parameter to facilitate comparisons. The characteristic time appeared to be the most useful parameter of those that are suitable for collision processes with both particles and surfaces. The characteristic time for an energy gain or loss is defined as the energy of an electron divided by the energy gain or loss rate,

$$\tau = \frac{E}{dE/dt}$$

When the energy gain or loss rate involves several collision processes, as is usually the case, the sum of the change rates is used:

$$\tau = \frac{E}{\Sigma(dE/dt)}$$

The energy loss rate is a result of soft, hard, exciting, and ionizing collisions of electrons with ions and of hard, exciting, and ionizing collisions of electrons with neutrals. At energies below about 1 ev, the soft collisions of electrons with ions are the major mechanism of electron-energy loss. Between 1 and 5 ev, the effects of hard collisions with ions and neutrals becomes increasingly important. From 5 to 10 ev, the losses are primarily by excitation. Above 10 ev, both excitation and ionization are important. Except at the lowest energies, where electron-ion collisions dominate, the number of neutrals has a strong effect on the losses. Different curves are therefore shown for ion-gage readings of 10^{-5} and 10^{-6} mm Hg.

The energy gain in sketch (b) results from collisions between electrons and ions. When the relative motion of the electrons and ions is viewed from the coordinate system of the ions, the motion is seen to be governed by plasma resistivity equations and results in ohmic heating of the electrons. Both soft and hard collision processes enter into ohmic heating, but the soft collisions are dominant up to about 30 ev. The electron and ion densities are not dependent on facility pressure, so only one curve is shown in sketch (b) for energy gain. There is, of course, a longitudinal potential gradient associated with this ohmic heating, but it is only of the order of 2 microvolts per centimeter at a 10-ev temperature.

If electrons were not gained or lost, the equilibrium electron energy would be that where the gain and loss times are equal. For both 10^{-5} and 10^{-6} mm Hg, the equilibrium electron energy or temperature would be about 5 ev. (This temperature assumes monochromatic electron energies. A different temperature would be obtained with a Maxwellian distribution, but the difference is negligible for the order-of-magnitude purposes of this analysis.)

To find the electron temperature for a more realistic situation, the gains and losses of electrons have to be considered. The gains are from ionization of neutrals and secondary emission from the target, and are shown in sketch (c).

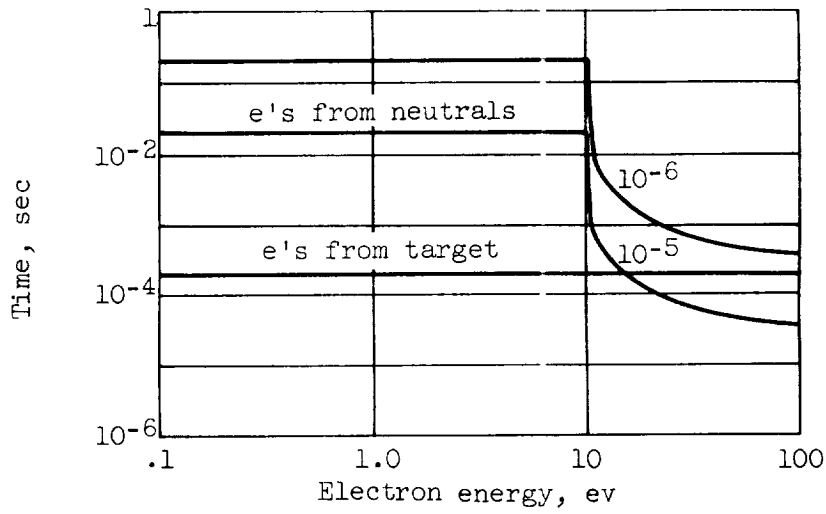

(c)

Again, characteristic time is plotted for a range of electron energy. The time for an electron addition process is the number of electrons in the beam divided by the rate of addition for that process.

The ionization of neutrals below an electron energy of 10 ev is by collisions of ions with neutrals; hence, it is not a function of electron energy. Above an electron energy of about 10 ev (the ionization potential of mercury is 10.4 ev), the electrons become more important than the ions in the ionization of neutrals, as shown by the rapid decrease in characteristic time. The ionization of neutrals, of course, introduces positive ions into the beam as well as electrons. These positive ions, though, are repelled from the beam by the same potential well that tends to contain the electrons. Ionization was assumed to take place in a single collision; that is, the possibility of successive collisions first exciting, then ionizing, was ignored.

The secondary emission from the target depends only on the ions and the surface, and hence is independent of both electron energy and neutral density. These secondary electrons leave the target with an initial energy that is a few percent of incident ion energy and thus may either be trapped or escape back to the target surface.

Rather than calculate the electron temperature for one special set of electron addition conditions, it is more in line with the objectives of this analysis to calculate the two limiting cases that might be encountered. The electron loss rate, which is discussed in the following section, is assumed equal to the addition rate for both cases. For the minimum temperature, consider the case where the electrons are almost entirely produced by collisions of ions with neutrals. That is, either the secondary electrons escape back to the target after a negligible time or else are suppressed entirely. The electrons from the neutrals will

have some energy as a result of the ionization process, probably of the order of ionization potential (10.4 ev for mercury). The equilibrium temperature can be found with the aid of sketch (d):

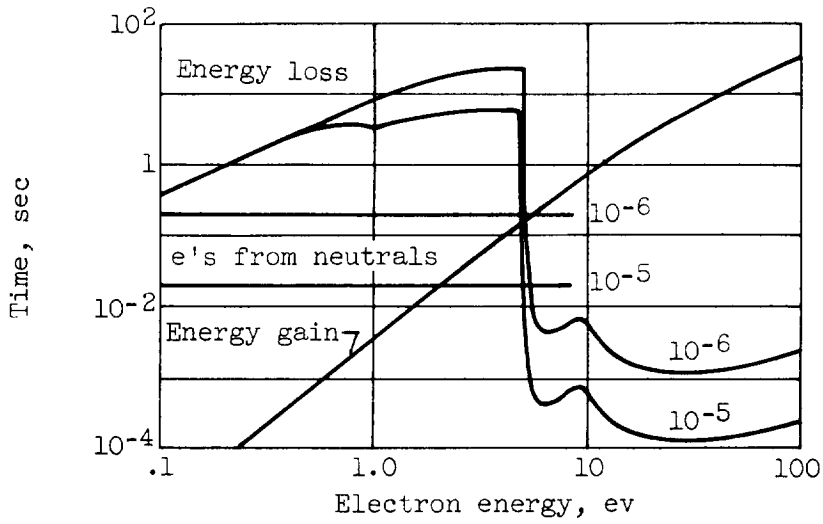

(d)

The energy loss and gain curves are the same as shown in sketch (b). That is, they show the effect of collisions on the energy of an electron, but they do not show the initial energy of an electron that is added or the final energy of an electron that is lost.

Above about 5 ev, the energy loss time is far shorter than either the electron addition or energy gain times, so that the initial electron energy is unimportant compared with the effect of collision processes. Thus, any electrons with more than 5 ev will be rapidly reduced to that energy level. Below 2 to 5 ev, depending on neutral density, the energy gain time is shortest - so that electrons will be heated. Thus, the equilibrium electron temperature should be somewhere between 2 to 5 ev when electrons are added only by collisions of ions with neutrals, which is roughly the same as was obtained without electron addition. In other words, the electron residence times are long enough for the minimum temperature case so that the same result is approached as with no electron addition.

For the maximum electron temperature to be expected, assume an initial electron population consisting only of secondary electrons from the target. Having come from the target, these electrons will initially possess a kinetic energy somewhat greater than the depth of the electrostatic well formed by the beam, perhaps 100 ev or more. Such electrons will almost certainly ionize neutrals and thereby produce additional electrons

at less kinetic energy. The well depth will be of the order of 100 volts or more, so that the low-energy electrons from neutrals will not be able to escape from the beam. Unless the low-energy electrons gain additional energy, they will accumulate and lower the mean temperature of the beam electrons regardless of the addition rate for high-velocity electrons. Whether or not these low-energy electrons will gain energy can be determined from sketch (e):

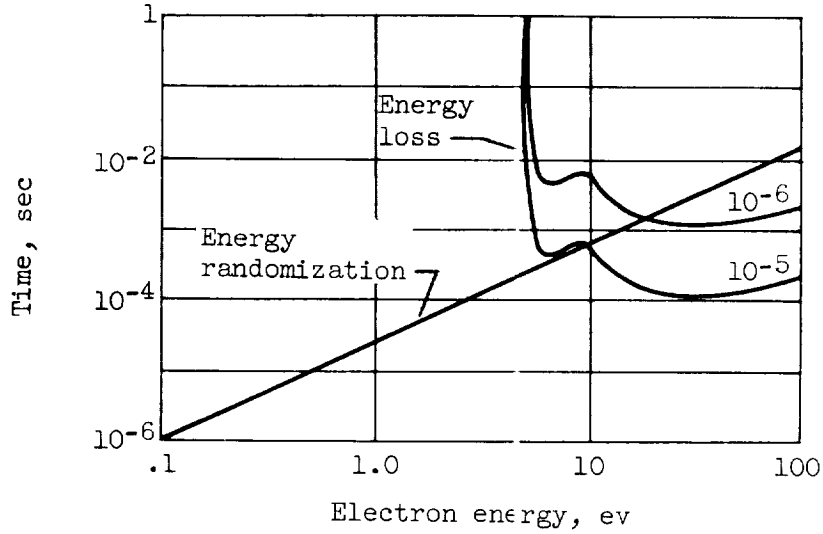

(e)

The energy transfer from high-energy to low-energy electrons is through the mechanism of soft collisions. The time for this process is shown by the "energy randomization" line in sketch (e). Since the energy randomization time is long compared with the energy loss time at high temperatures, it is evident that the low-energy electrons will approach 5 to 20 ev, depending on neutral density. Thus, the low-energy electrons should accumulate and lower the mean electron temperature in the beam to 10 or 20 ev as a maximum temperature. The energy gain due to ions heating the electrons is not shown in sketch (e), but the energy randomization process has a much shorter characteristic time.

The electron loss rate was assumed equal to the addition rate in the electron-temperature analysis. It is worthwhile to examine what is involved in this loss rate. The loss of electrons from the beam is by recombination and escape of the high-velocity Maxwellian "tail". Radiative recombination is the primary mode of recombination at ion-beam densities. The time for such recombination is many orders of magnitude greater than that for electron production processes, as is shown in figure 1 where times for the various collision processes are summarized.

E-1720

Thus, the major process to consider for electron loss is escape through the sheath to the target. The electrostatic well depth necessary to keep the loss rate equal to the addition rate can be calculated quite simply if a Maxwellian distribution is assumed. For the 2-ev minimum temperature the well depth should be 25 to 30 volts, depending on neutral density. (The calculation method is shown in the appendix.) For the maximum temperature of 20 ev, the well depth should be about 210 volts. The well depth for the 2-ev temperature is probably reasonable because the energy randomization time is shorter than any other time, which results in a close approach to the Maxwellian distribution. For the 20-ev temperature the Maxwellian "tail" would probably be attenuated, because the energy loss time is less than the energy randomization time above 20 ev (sketch (e)). Thus, the 210-volt depth is probably too large.

To compare theory with experimental results, the source of sparking at low neutral densities should be found. The obvious cause of sparking is that the local breakdown gradient is reached. Admittedly, the breakdown gradient is low under ion bombardment - only a few thousand volts per millimeter from some accelerator experience, but the sheath gradients (200 volts across several millimeters) do not begin to approach breakdown values. Thus, the sparking cannot be explained in terms of collision processes.

To summarize the results of the collision-process analysis, the electron temperature in an ion beam should be 2 to 20 ev when no neutralizer is used in a test facility. The electrostatic well depth necessary to keep the electron loss rate equal to the addition rate should be between 25 to 200 volts. The results from this simple model clearly do not explain the sparking phenomena. It is true that both the model and experiment indicate stable performance at 10^{-5}. But the model also predicts stable performance (for the same reasons) at 10^{-6} mm Hg, where sparking problems are encountered. Also, measured potential gradients in the beam are far too large to be explained by simple collision processes, and considerable evidence for wave phenomena exists - as is shown in the next section. The collision-process analysis presented is the steady-state approach to plasma behavior. Since the experimental results cannot be explained with such an approach, the next step is to consider transient phenomena.

Plasma Waves

When an ion engine is operated without a neutralizer in a test facility, the electrons are confined in an electrostatic well while the ions pass through them. The relative motion between the ions and electrons is capable of supplying energy for the production of plasma waves. A very brief introduction to plasma waves (in the absence of magnetic fields) is included to aid those who are unfamiliar with such phenomena. Reference 8, from which much of this material was extracted, is suggested for further reading.

There are two main types of plasma waves to consider in experiments with negligible magnetic fields, such as ion beams. One is the electron-plasma wave, where the changes occur so rapidly that the ions are effectively stationary. The frequency of this oscillation is given by

$$f_- = \sqrt{\frac{n_- q_-^2}{\pi m_-}} = 8.98 \times 10^3 \sqrt{n_-}$$

where n_-, q_-, and m_- are the electron number density (per cc), charge, and mass. For an electron density of 10^9 per cubic centimeter, the electron-plasma frequency would be about 284 megacycles per second. Electron-plasma waves are strongly damped (Landau damping) when the phase velocity (velocity of a single cycle) is less than mean thermal velocity. There are theoretical reasons for expecting a range of electron-plasma frequencies extending down from f_-, but frequencies much below f_- correspond to low phase velocities and hence strong damping. In reported plasma literature, frequencies have been found in a narrow band near f_-. Such frequencies are assumed to be electron-plasma oscillations.

The other type is the ion-plasma wave, where the changes are so slow that the electrons continuously adjust to the Boltzmann distribution. For very short wavelengths the ion-plasma frequency is

$$f_+ = f_- \sqrt{\frac{m_-}{m_+}}$$

where m_+ is the ion mass. For mercury ions at a density of 10^9 per cubic centimeter, f_+ would be about 468 kilocycles per second. For long wavelengths the frequency is

$$f^2 = \frac{f_+^2}{1 + \left(\frac{\lambda}{2\pi l_D}\right)^2}$$

where λ is the wavelength and l_D is the Debye shielding distance, which is defined

$$l_D = \sqrt{\frac{q_- \bar{V}_-}{4\pi n q_-^2}} = 7.43 \times 10^2 \sqrt{\frac{q_- \bar{V}_-}{n_-}}$$

The electron temperature $q_- \bar{V}_-$ is in ev (temperature in $^\circ$K divided by 11,605). For long wavelengths the phase velocity approaches the limiting value of $2\pi f_+ l_D$. This velocity varies as the square root of electron

temperature but would be about 2.2×10^5 centimeters per second at 10 ev and a density of 10^9 per cubic centimeter. In reported plasma literature, broad ranges of frequencies extending downward from f_+ have been observed. These frequencies are presumably caused by ion-plasma oscillations.

According to the theoretical study in reference 9, the drift velocity (ordered relative motion between electrons and ions) should be about equal to the electron thermal motion $\sqrt{2q_-\bar{V}_-/m_-}$ before electron-plasma waves are amplified. This velocity would be about 1.9×10^8 centimeters per second for 10-ev electrons. Electron-plasma oscillations would be prevented at lower drift velocities by Landau damping. The corresponding threshold for ion-plasma-wave amplifications depends on ion random energy. For equal electron and ion random energies (temperatures), this threshold is about the same as for electron-plasma waves. For ion random energies much less than electron random energies, which is the case most likely to be encountered in an ion-rocket beam, the threshold for drift velocity is approximately $\sqrt{2q_-V_-/m_+}$. This velocity is lower than electron thermal velocity by the square root of electron-to-ion mass ratio. For mercury ions and 10-ev electrons, this velocity would be about 3.1×10^5 centimeters per second.

Some interesting calculated results are presented in reference 10 for the case where the electron drift velocity initially exceeds the threshold for electron-plasma-wave amplification. Electron-plasma waves were found to be amplified to the point where the electron drift velocity is rapidly randomized. Thus, an ordered electron motion could be rapidly translated into a rise in electron temperature. This randomization usually occurred in about 30 plasma wavelengths, which would be somewhat less than 1 centimeter for 10-ev electrons and densities of 10^9 per cubic centimeter. It was predicted that drift velocities of even "runaway" magnitude would be stopped in about 100 electron-plasma wavelengths.

To return to ion-rocket experiments, the first thorough study of transient phenomena in an ion beam was presented in reference 2. A repetitive wave phenomena was found with a frequency closely related to transit time for the ions. A search for signals of electron-plasma frequency yielded negative results.

A brief related investigation was made at Lewis following the publication of reference 2. Thin wires were strung across the path of an ion beam in one of the 5-foot-diameter, 16-foot-long vacuum tanks as shown in sketch (f).

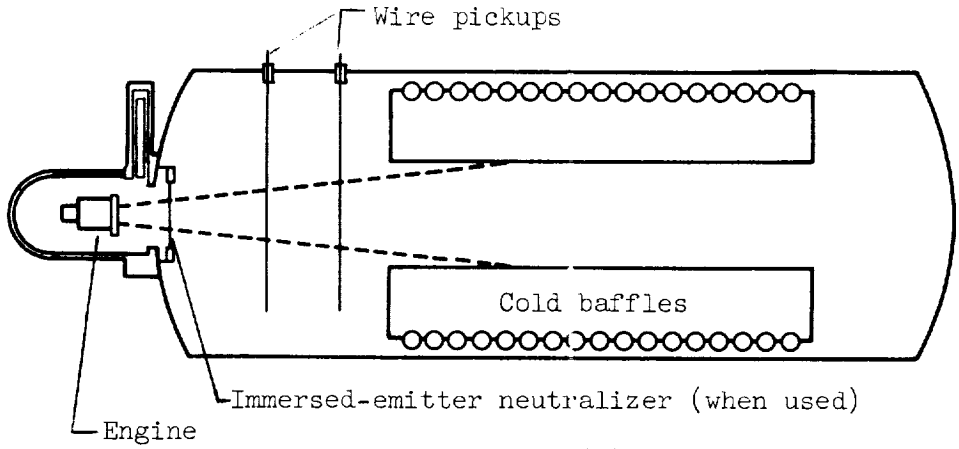

(f)

The wires were insulated from the tank and served as electrical pickups for the longitudinal potential gradient. Because of the high electron random velocity, the wire pickups tended to accumulate a negative charge, so that the absolute potential had only a vague relation to plasma potential. The charge buildup on both wires should be about the same, however, so that the potential difference between the two wires should at least give a rough indication of the true potential difference in the plasma. The mean distance of the wires from the engine was about 1 meter, although the overall beam length was substantially greater.

An ion rocket with an electron-bombardment ion source was operated with a 0.125-ampere ion beam at a specific impulse of 5000 seconds. The neutral density was varied to give ion-gage readings from about 3×10^{-6} to 3×10^{-5} mm Hg. As far as the overall engine measurements of voltages and currents were concerned, the operation appeared stable. The longitudinal potential gradients in the beam, as indicated by the pickup wires, are shown in sketch (g):

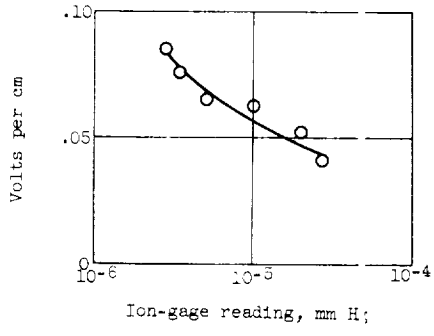

(g)

The direction of the gradient, with the upstream wire being more positive, was the same as would be expected for soft collisions between electrons and ions. The magnitude of the measured gradient, however, was too big by a factor of at least 10^5.

Alternating-current signals from the pickup wires were also investigated. Using several instruments, a range of frequencies from about 10 cycles per second to 400 megacycles per second was investigated. Signals were found over a broad range of frequencies from less than 1000 to over 20,000 cycles per second. The maximum amplitude of these signals from the pickup wires was several tenths of a volt at roughly 10,000 cycles per second. When viewed on an oscilloscope, the a-c signals had no apparent repetitive structure. No clear indications of other signals were found. The background noise with the engine off, however, was quite high in the megacycle range, and signals of as much as 10-microvolt amplitude might have been masked by noises at some frequencies.

The signals in the kilocycle range were assumed to be from ion-plasma waves. Comparison of threshold drift velocities with ion velocity supports this conclusion. The threshold drift velocity for ion-plasma-wave amplification is far less than ion-beam velocity, while that for electron-plasma waves is far greater.

There are two ways in which ion-plasma waves could drag electrons along with the ions and produce the large potential gradients shown in sketch (g). The first is simply trapping electrons in the waves. Since the propagation velocity of such waves is much less than ion velocity, the waves would be carried at essentially ion velocity.

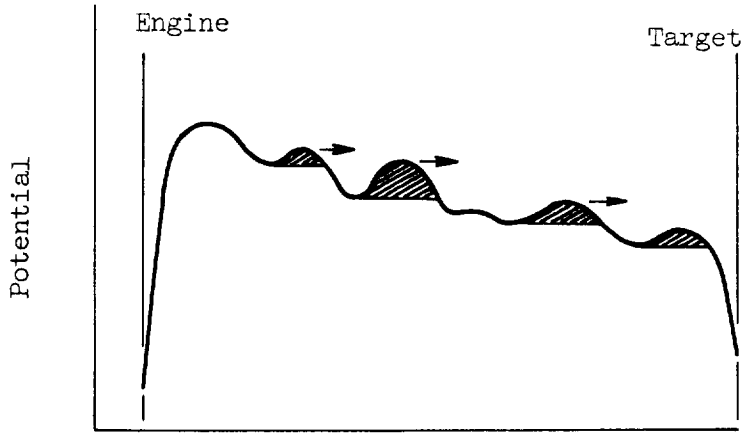

(h)

These ion-plasma waves would form traps (shaded portions in sketch (h)) to carry the less energetic electrons along with the ions.

The second way in which electrons would be dragged along with the ions is through scattering effects of ion-plasma waves. The resistivity of a plasma results from the randomization of the drift velocity. For low drift velocities this randomization is, of course, accomplished by simple collision processes. Randomization, though, can also be caused by potential gradients in the plasma, so that the effects of ion-plasma waves may far overshadow the simple collision processes considered previously.

The effect of neutral density on ion-plasma waves should be primarily through electron production rate. At the highest neutral density in sketch (g), the electron production rate should be almost sufficient to current-neutralize the beam at the pickup wires. Only a small percentage of the electrons carried to the target by ion-plasma waves would have to return upstream to maintain equilibrium. The mean relative velocity between the electrons and ions would, therefore, be low. As the neutral density is decreased, the electron production rate in the beam decreases, and the mean relative velocity between electrons and ions approaches ion velocity. The sparks at low neutral densities could be attributed, therefore, to the large electron-ion coupling at large relative velocities. Since the electrons would be expected to be carried downstream, the relative velocity between electrons and ions should be greatest near the engine. Thus, the potential gradients in sketch (g) may be much less than those nearer the engine. It is not clear, however, whether the sparks are caused entirely by static potentials in the beam or whether large-scale transients are also important.

To reexamine the phenomena in reference 2 in the light of plasma-wave theory, it appears that an ion-plasma wave, or waves, carries electrons toward the target. When enough electrons have been carried downstream and the longitudinal electric field reaches a sufficiently high value, the electrons that have not escaped to the target rush back to make the beam potential more uniform. After a short period when the beam potential decreases because of electrons being added to the beam faster than they are escaping to the target, the wave - or waves - again starts carrying electrons downstream. The lack of sparks as compared with operation at Lewis was probably due to the lower accelerator voltages and shorter beam lengths, so that the breakdown potential difference simply was not reached. The constant frequency of repetition as compared with the almost-random phenomena observed at Lewis was probably due to a well-defined beam length. That is, the target was placed transverse to the beam so that the beam ended at a definite distance from the ion accelerator. In the Lewis experiments, the beam ended on cold baffles that extended over much of the tank length - making an exact beam-length measurement impossible.

In summarizing, it appears that all the major features of ion-beam behavior without neutralizers can be explained qualitatively with plasma-wave theory. The relative motion of electrons and ions generates plasma

waves, although the frequencies observed indicate that only ion-plasma waves have been present. The trapping and the scattering effects of such waves could explain the large observed coupling between electrons and ions. The absence of electron-plasma frequency signals is presumably due to the low ratio of drift to thermal motion for electrons.

The apparent effect of ion-plasma waves on electron-ion coupling suggests an interesting experiment. One or more engine electrodes could be modulated at various frequencies. This modulation might augment the natural amplification to produce even larger waves and greater electron-ion coupling effects.

OPERATION WITH NEUTRALIZERS IN TEST FACILITIES

A variety of electron-ion interaction phenomena have been indicated by the analysis of operation without neutralizers. The next step is to examine operation with neutralizers to see if the same phenomena are present. The first neutralizer considered is the immersed-emitter type.

Immersed-Emitter Neutralizer

The longitudinal potential variation for an ion rocket employing an immersed-emitter neutralizer is shown in sketch (i):

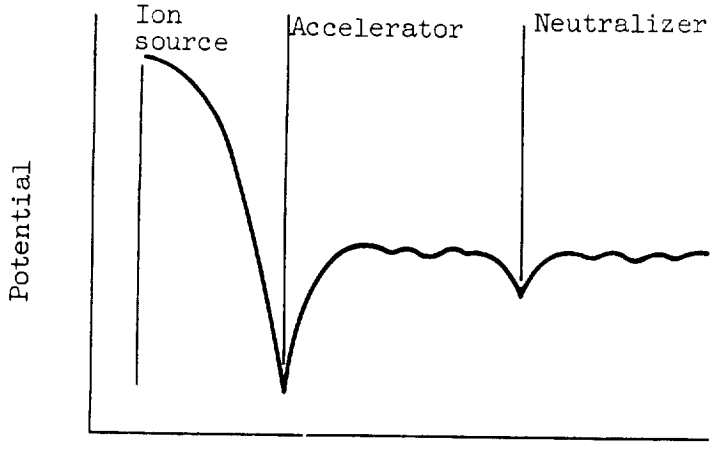

(i)

The acceleration is accomplished between the ion source and the accelerator. The ion source can be either a hot surface (in a contact-ionization engine) or a plasma sheath (in an electron-bombardment engine). Some accel-decel is desirable to keep the beam electrons out of the ion accelerator, so a deceleration region is shown between the accelerator and the

ion beam. This deceleration can be accomplished by using a decelerator electrode or, as shown in sketch (i), by letting the upstream end of the beam act as a virtual decelerator electrode. The potential of the beam is presumably set by the neutralizer, so the neutralizer might be considered the decelerator in the configuration of sketch (i). A small potential difference is shown between the neutralizer and the beam to overcome local space-charge effects near the neutralizer. This potential difference should be small to keep the electron velocity small; but, at the same time, the emitter area should be small to keep the sputtering rate small. These two objectives are not in accord. Practical designs that compromise these two objectives will probably have minimum electron energies of a few ev.

The regulation of electron current should be accomplished by variations in the potential difference between the neutralizer and the beam. For example, if too many electrons leave the neutralizer, the potential difference between it and the beam decreases. If space-charge-limited electron current is assumed, the decrease in potential difference should decrease the electron current and restore the balance between electron and ion currents. As is shown by the experimental data presented next, the immersed-emitter neutralizer may or may not behave in this manner, depending on the potential difference between the target and the neutralizer.

The immersed-emitter neutralizer used in the Lewis experiments was simply a thin tantalum wire stretched across the path of the ion beam, as shown in sketch (f). The pickup wires described in the preceding section were also used in conjunction with the neutralizer. As mentioned in reference 7, the initial use of this neutralizer was to reduce sparking at low pressure. The longitudinal potential gradients indicated by the pickup wires were recorded with the neutralizer operating, as shown in sketch (j):

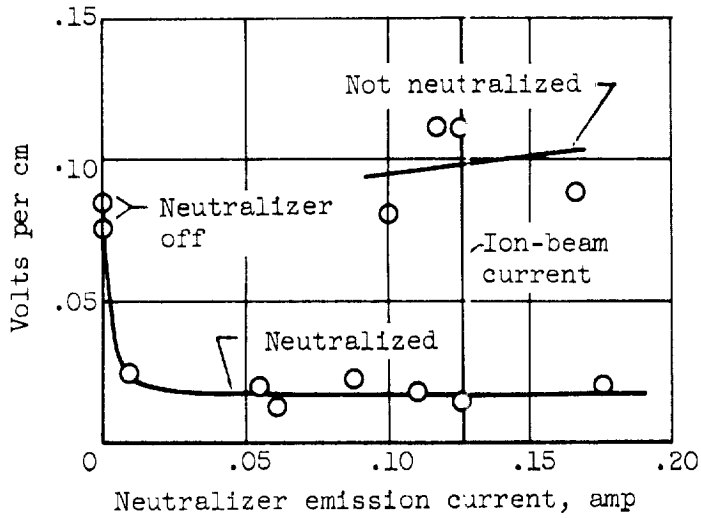

(j)

These data were obtained at an ion-gage reading of about 3×10^{-6} mm Hg. With the exception of the two points with the neutralizer turned off, all the data were obtained at constant heater current with the emission current changed by varying the neutralizer potential relative to the test facility. Two modes of operation were found. The "neutralized" mode gave the lower potential gradients and was obtained with neutralizer potentials from about +10 to -20 volts. The "not neutralized" mode with higher potential gradients was obtained with neutralizer potentials from about -10 to -100 volts. The first mode is the operation that might be expected from the results of the previous section. Addition of electrons reduces the electron-ion relative velocity, and hence the coupling between the two. Reduced electron-ion coupling was also indicated by a reduction in amplitude of the kilocycle-range a-c signals when the neutralizer was turned on - by more than a factor of 10. The rapid decrease in potential gradient with small neutralizer currents indicates a highly nonlinear relation between coupling and relative velocity. The "not neutralized" mode apparently is the same as that reported previously in reference 2, with the electrons from the neutralizer passing directly to the target. The interaction between ions and the trapped electrons, as indicated by the potential gradients, is apparently unaffected by the neutralizer electrons under such conditions. The kilocycle-range signals for this mode were substantially the same as that with the neutralizer off, which also indicated negligible effect of the electrons from the neutralizer.

The megacycle-per-second range was also investigated with the neutralizer on. Signals of the order of 50 microvolts maximum amplitude were found of several frequencies from about 200 to 300 megacycles per second. These signals were assumed to be electron-plasma oscillations and corresponded roughly to the electron densities near the neutralizer. The amplitudes of these signals were approximately zero when the neutralizer was positive to, or nearly the same potential as, the rest of the facility. The amplitude increased as the neutralizer was made more negative until, after reaching a maximum amplitude at -10 to -60 volts, it decreased slowly with further potential decreases. Some other signals were found in the 35- to 40-megacycles-per-second range. These signals showed a similar amplitude variation with neutralizer bias except that the maximum amplitude was about 1 millivolt. This lower frequency range corresponded roughly to the expected density range for the high-velocity electrons that would go directly from the neutralizer to the target.

One other experiment at Lewis should be mentioned. In the early work, before the need for low electron velocities was fully appreciated, neutralization was attempted with 200-ev directed beams from electron guns. Such directed streams of electrons entering the ion beam would be expected to have a large directed velocity compared with the electrons trapped in the beam.

A folded dipole was placed inside the vacuum tank, parallel to the beam. Signals of about 25-megacycles-per-second frequency and harmonics thereof were detected. The fundamental had the largest amplitude, which was about 30 microvolts. Calculation indicated that this frequency corresponded to electron-plasma frequency for an electron density about that of the electron beams. This is the only other ion-rocket experiment known to the author in which waves of this frequency were clearly detected. The engine operated with no ill effects, and the experiment is mentioned merely to indicate what might be expected at very large electron directed-to-random velocity ratios.

To return to reference 2, the immersed-emitter neutralizer used was an oxide-coated button in contact with the side of the ion beam. As mentioned in connection with the Lewis experiments, most of the neutralizer electron current apparently passed directly to the target while contributing little to the charge neutralization. Even so, the oscillatory behavior observed without a neutralizer was usually absent with a neutralizer, which indicated some degree of stabilization.

Some interesting ion-energy spectrums were also shown in reference 2. When the beam was in an oscillatory condition, the ion-energy spread was roughly 100 ev for a mean value of 700 ev. This spread of ion energies was reduced to a negligible value in the absence of oscillations.

The major advantage of the immersed-emitter neutralizer is, of course, simplicity: no complex electrodes or delicate potential adjustments - just a simple electron emitter. The price that must be paid for this simplicity is sputtering erosion. This erosion can be reduced by moving the emitter to the edge of the beam where the ion-current density is less. The exact point where the electron density is too low to serve as an effective conductor to the rest of the beam will probably have to be determined by experiment.

Electron-Trap Neutralizer

The essential part of an electron-trap neutralizer is a potential well. This potential well is shaped by electrodes. Grid electrodes could presumably be used to establish the desired potential variation in a broad beam (a beam whose width or diameter is large compared with Child's law accelerating distance). Such grids, however, would be subject to sputtering erosion, which would thus cancel perhaps the most important advantage of the electron-trap neutralizer. Thus, electrodes outside of the beam should be used to shape the potential variation within the beam. For the effect of the electrodes to be felt within the beam, the electron-trap neutralizers must be limited to thin beams. This does not mean that such a neutralizer will not work with large ion-beam currents. It means instead that a neutralizer for large ion-beam currents should be constructed of many small elements, with each of these elements neutralizing a small fraction of the total beam.

The longitudinal potential variation for an ion rocket employing an electron-trap neutralizer is shown in sketch (k):

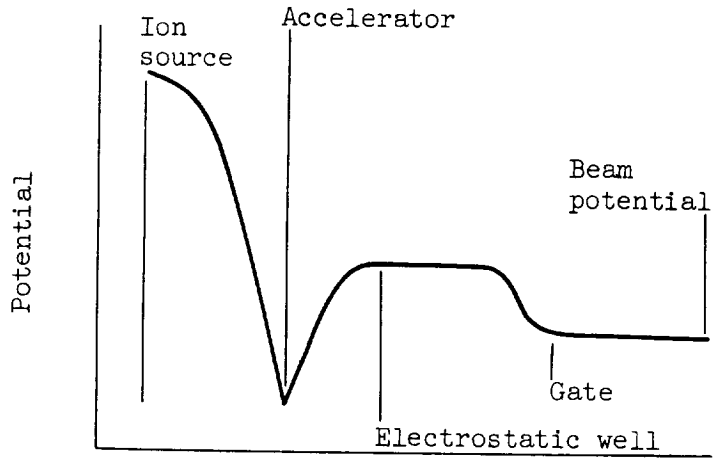

(k)

As in the case of the immersed-emitter neutralizer, the use of accel-decel provides a potential barrier to prevent electrons flowing back through the ion accelerator. The electrostatic well to trap electrons is immediately downstream of this barrier. The electrons are emitted into this well, the emitter potential being close to beam potential. The well depth, which is the potential difference available to overcome space-charge effects between the emitter and the ion beam, is usually several volts. The gate for controlling electron departure rate is at the downstream end of the well.

The electrons are emitted into the well at a uniform energy of a few ev with a small thermal energy distribution superimposed. This thermal distribution comes from the electron emitter and has a magnitude of 0.1 to 0.2 ev.

References 4 and 5 both indicate that the trapped electrons may lose sufficient energy to reduce their random velocity to the order of the ion directed velocity. The possibility of such energy losses, however, can be disproved in a quite general manner. In the range of interest of several ev, or less, electron random energy can be reduced only by increasing ion random energy a like amount. From the equipartition law, with the equality of electrons and ions that would be expected with current neutralization, the most that the electrons can lose is half of their initial random energy. Beyond that point the ions would tend to increase electron random energy. The minimum initial random energy would be about 0.1 ev, but the required electron random energy for a velocity of 4.9×10^6 centimeters per second, for example, is less than 0.001 ev. To be sure, the possibility of a dumbbell or other odd-shaped ion molecule might theoretically permit slightly more than half the electron

random energy to be lost, but the resultant energy would still be far from that required. All this does not mean that electron velocities as low as that of the ions cannot be achieved. It simply means that it should not be expected as the result of any energy loss process in a trap.

Now that the theoretical limit of trap processes has been discussed, it is of interest to consider what may reasonably be expected to occur in the trap. The ion residence time in a 1-centimeter trap will be less than a microsecond for any ion velocity of interest for a space mission. If current neutralization and equal electron and ion densities in the trap are assumed, the residence time of an electron will be the same as that of an ion. In comparing this residence time of less than 1 microsecond with the collision-process times in figure 1, it should be evident that collision processes can be ignored - even if the densities and trap dimensions were increased by an order of magnitude. The ratio of drift to random velocity should be small enough in the trap to preclude the possibility of electron-plasma oscillations. Also, the tendency of external electrodes to fix potentials in the trap may suppress ion-plasma waves. Thus, with the possible exception of ion-plasma waves, there should be no significant randomizing effect in the electron trap.

With negligible randomizing effects and a simple barrier effect at the gate, the electron random energy in the beam should be about the same as that from the emitter, 0.1 to 0.2 ev. Ion-plasma waves could increase this random energy to as much as several ev for waves whose amplitude was about equal to well depth.

There is another way to reduce electron temperature in the beam: by shaping the gate at the exit of the well. The upstream side of the gate can be a gradual slope as shown in sketch (2):

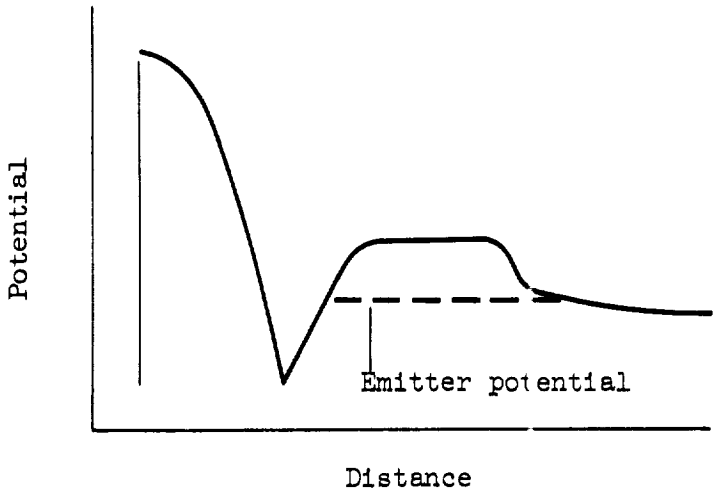

(2)

With the emitter set at the potential shown, the electrons approaching the gate would be reflected in the region where the potential change with distance is gradual. The reflected electrons will have a variety of transverse velocities. Those with transverse velocities near zero will almost completely stop before being reflected. But the soft-collision cross section becomes very large at very low velocities, and such electrons would tend to be carried along with the ions. If the slopes were sufficiently gentle at the gate, only very low velocity electrons (plus a negligible number with very high velocities) would find their way into the beam. To illustrate the temperature selective nature of such a gate design, 0.01-ev electrons could be carried against an adverse potential gradient of more than 0.02 volt per centimeter by soft collisions with ions whose density is 10^9 per cubic centimeter, while 0.1-ev electrons could only be carried against slightly more than 0.001 volt per centimeter. This effect would be almost proportionately greater for higher ion densities.

The regulation of electron current in an electron-trap neutralizer is a two-step process. The electron density in the well partially determines the potential of the well and hence the value of the space-charge-limited electron current from the emitter to the well. In a similar fashion the electron density in the beam partially controls the gate potential (both the height and slope), and hence the electron current to the beam. The potentials of the well and gate, however, are also determined in a large part by external electrodes. The potential variations that can be caused by electron-density changes are quite limited. The initial settings of electrode potentials must therefore be quite close to the required values before the neutralizer can become self-regulating.

The preceding discussion of the electron-traps neutralizer is mostly speculative and theoretical. The available data for this type of neutralizer are not sufficient to determine which of a variety of theories is (or are) supported by experimental results. It is hoped that future experimental work will clarify the situation.

OPERATION IN SPACE

Most ion rockets for space applications will have much larger ion-beam currents than present experimental models. The corresponding aspect ratios (beam diameter divided by Child's law accelerating distance) will be very large. Such ion beams will undoubtedly be made up of many small beams. Neutralization can be approached by separately neutralizing each of the small beams or, using one large device, neutralizing the aggregate beam. If an electron-trap neutralizer is to be used, then the former approach should be used. The advantages of such a neutralizer would be, of course, low sputtering erosion and perhaps low electron temperature. For an immersed-emitter type of neutralizer there is no advantage to be

gained by neutralizing each of the elemental beams. The inherent simplicity of a single large neutralizer (or at most just a few neutralizers) should make that course more desirable. The advantages of an immersed-emitter neutralizer would then be simplicity and probably a reduced power loss. The latter stems from the smaller total electron-emitter area that can probably be used in one large neutralizer.

Ion rockets have been operated many hours in test facilities. The expectations in space must be based in part upon such operation. To date, there has been no indication of an instability that would prevent operation of an ion rocket in space. In fact, there is evidence to the contrary. The wave phenomena that tend to reduce relative motion between electrons and ions should help damp out departures from neutrality.

A point of particular concern is the initial neutralization that is required when an ion rocket is first started in space. Starting from a non-neutralized condition, the beam will have a large positive potential relative to the neutralizer, as shown in sketch (m):

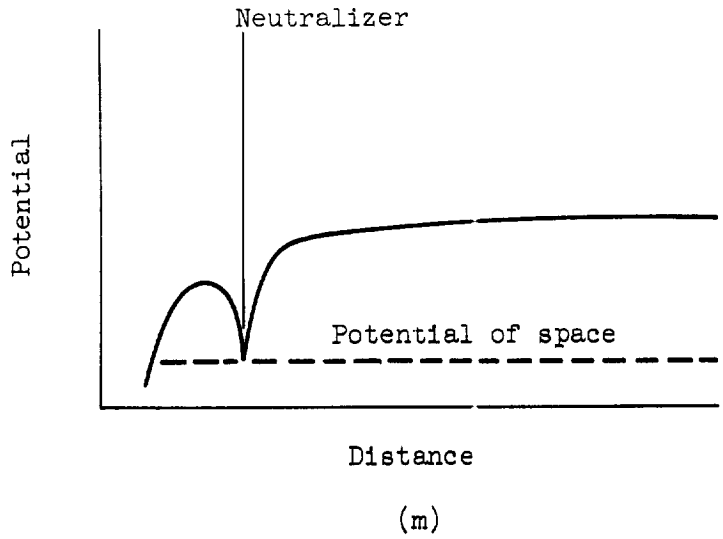

(m)

An immersed-emitter neutralizer is indicated in the sketch, but the reasoning applies equally well to operation with an electron-trap neutralizer. The beam potential should draw an electron current far greater than that required for current neutralization. Ignoring plasma-wave interactions that would help neutralization, the beam potential should accelerate these electrons to a high velocity so that the charge density of the beam is unaffected. After a few microseconds of this high electron current, the space vehicle should reach a positive potential sufficient to limit electron current, as indicated in sketch (n).

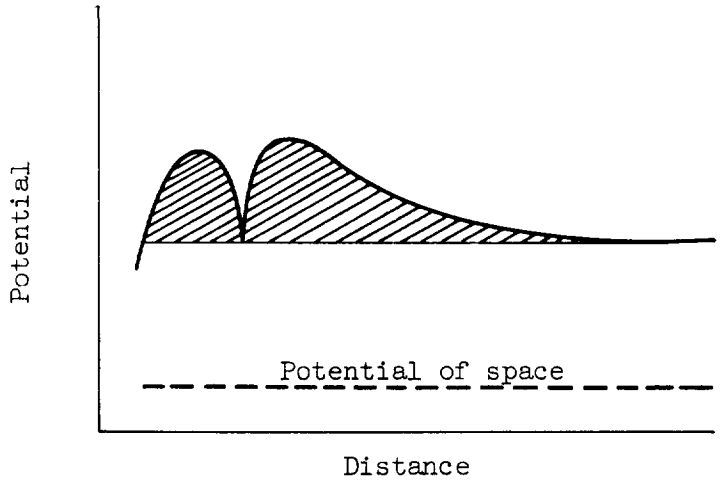

(n)

An electron trap is thus formed. Collision processes with ions and the few neutrals that escape from the engine should reduce the trapped electron velocities to several ev in a few milliseconds. With the accumulation of trapped electrons the beam should approach a final value within a few volts of the potential of space (the potential far from any charged body) and neutralization. The initial non-neutralized condition may exhibit turnaround for a few milliseconds if the beam is started at a high ion current. The experiments described in reference 2 indicate that such a transient initial condition should not be harmful.

The development of large ion-rocket-propelled space vehicles, however, requires more than the vague expectation of success. If possible, more certain indications should be obtained from Earth-bound facilities. There appear to be two requirements for accurate simulation. The first is that the neutral density be sufficiently low. The tendency of ion-plasma waves to carry low-velocity electrons along with the ions eases the neutral density requirement. As long as the electron production rate from residual neutrals is small compared with the ion-beam current, the neutral density simulation should be adequate.

The other requirement is that the boundaries of the test facility be sufficiently removed that their effects are small. A distance of a few beam diameters will suffice in most directions. The target, though, presents a greater problem. The beam, being a conducting plasma, serves to couple the target and engine. The target could presumably be connected to circuitry that would approximate the impedance of an infinite beam, but such an approach appears to be beyond the present state of knowledge. The only approach that offers much hope for the near future is separating the engine and target by a large distance. If the beam has sufficient impedance, then the presence of the target should have little effect on

operation. The adequacy of beam impedance for space simulation could be determined by varying the target potential. For example, if the target were varied by 1 percent of the electron thermal potential $\overline{V}_-$, then the beam impedance would probably be adequate if operation of the engine was not impaired and the electron-beam current varied by only 0.1 percent or perhaps 0.01 percent. The beam impedance would, of course, have to be investigated for transients and a-c variations as well as slow d-c changes.

CONCLUDING REMARKS

Soft collisions and hard two-body collisions are the coupling mechanisms between electrons and ions at very low drift velocities. Ion-plasma waves apparently form, however, at the drift velocities encountered in test facilities. The trapping of low-velocity electrons in such waves and carrying them along at essentially ion velocity, together with the scattering effects of such waves, would explain the large apparent electron-ion coupling observed. There is some experimental and theoretical evidence for believing that very large electron-ion velocities (as large as, or larger than, electron random velocity) would cause electron-plasma waves that would rapidly randomize the drift velocity.

The present state of knowledge concerning such plasma waves in ion-rocket beams does not go much beyond identifying the general type of phenomena. The importance of plasma waves in beam behavior should serve as ample incentive to obtain more precise knowledge in this area.

The general effect of such waves should be to aid rather than hinder neutralization. That is, the electron-ion coupling should serve to damp out departures from neutrality. Ion-plasma waves also have such low propagation velocities that they should be swept away from the ion rocket in space and thus not impair operation. Such is not the case with electron-plasma waves; but, in the experiments where such waves were found to be present, the performance of the ion rocket was not adversely affected.

It does not appear easy to prove that neutralization will work in space without actually putting an ion rocket in space. The most critical test for simulation of space operation in an Earth-bound facility appears to be that for beam impedance. If variations in target potential cause only second-, or third-order changes in engine operation, then the beam impedance should be sufficient to isolate the engine from the target. Such impedances may unfortunately require impractical beam lengths.

As for the type of neutralizer that should be used on a space mission, both the electron-trap and immersed-emitter types have advantages. With the uncertainties that exist about operation in space, it would certainly be too early to decide which advantage or advantages will prove to be more important. Also, there is more than one type of ion rocket, so that both neutralizer types may prove advantageous in different applications.

Lewis Research Center
National Aeronautics and Space Administration
Cleveland, Ohio, May 29, 1961

APPENDIX - COLLISION PROCESSES

The characteristic times for collision processes in an ion beam are presented in figure 1. The data sources and assumptions necessary for the calculation of these times are presented in this section. Because of the order-of-magnitude nature of this analysis, the values in figure 1 should be used as only a rough approximation.

Electron Escape to the Target

The electrons escape from the beam to the target through the adverse potential gradient of the sheath surrounding the target. The equation for the electron arrival per square centimeter of target $\dot{n}_-$ is

$$\dot{n}_- = \frac{n_- \bar{v}_-}{2\sqrt{\pi}} e^{-\Delta V/\bar{V}_-}$$

with n_- the electron density per cubic centimeter in the beam, $\bar{v}$ the electron most-probable velocity, ΔV the potential difference across the sheath, and $\bar{V}_-$ the thermal potential. The most-probable velocity is obtained from

$$\bar{v} = \sqrt{2q_-\bar{V}_-/m_-}$$

Secondary Emission

The secondary-emission coefficient was obtained from reference 11. The values for all available ions except hydrogen and helium, moving at a velocity of 4.9×10^6 centimeters per second, ranged from about 0.01 to 0.1. With the comparatively dirty surfaces to be found in a test facility as opposed to a carefully prepared test specimen, the higher value was felt to be appropriate. For cesium ions impinging on a cesium-coated surface, another factor of 10 in secondary emission might be expected. With γ as the secondary emission coefficient and v_+ the ion velocity, the secondary emission per square centimeter of target $\dot{n}_-$ is simply

$$\dot{n}_- = \gamma n_+ v_+$$

The characteristic time for secondary emission is

$$\tau = \frac{n_- l}{\dot{n}_-}$$

with l the length of the beam in centimeters.

Radiative Recombination

Radiative recombination is the major method of recombination at the pressures encountered in ion-rocket test facilities. The recombination coefficients for radiative recombination were obtained from reference 12. The recombination coefficient can be used to calculate a recombination cross section σ_r, so that recombination calculations can be made on the same basis as those for most of the other collision processes:

$$\sigma_r = \frac{\alpha}{\bar{v}_-}$$

The radiative-recombination cross sections thus calculated from reference 12 are:

Temperature, ev	0.1	1.0	10	100
Cross section, cm^2	1.1×10^{-19}	7.0×10^{-21}	3.5×10^{-22}	1.1×10^{-23}

The radiative-recombination rate per cubic centimeter, assuming equal electron and ion densities, is

$$\frac{dn_-}{dt} = \sigma_r n_-^2 \bar{v}_-$$

The characteristic time is, of course,

$$\tau = \frac{n_-}{(dn_-/dt)}$$

Soft Collisions

Reference 12 was the original source for the soft, or coulomb, collision cross sections and the plasma resistivity equation. This information, however, was also presented in the appendix of reference 7 in a form more convenient for these calculations. The plasma resistivity equation was used, together with the soft-collision cross section to calculate the heating rate for electrons trapped in a test facility with an ion beam passing through them. Above about 10 ev, the ion hard-collision cross section had to be added to the soft-collision cross section for the resistivity calculation.

The soft-collision cross section was also used for an approximate calculation of energy-randomization time,

$$\tau = \frac{1}{\sigma_s n_- \bar{v}_-}$$

If the energy randomization time is short compared with other times, then a Maxwellian distribution is approached.

The final soft-collision cross section used was that for energy exchange from electrons to ions. This soft-collision cross section is lower than the preceding values by the ratio of electron mass to ion mass. The rate of energy loss for these collisions is, in ev per electron,

$$\frac{dE}{dt} = \sigma_s \frac{m_-}{m_+} n_+ \bar{v} \, (q_- \bar{V}_-)$$

This loss, together with other collision losses, is used to calculate the characteristic time for energy loss,

$$\tau = \frac{q_- \bar{V}_-}{\Sigma(dE/dt)}$$

Hard Collisions

References 13 and 14 were the original sources for the hard, or large-deflection, collision cross section of electrons with mercury atoms. Below about 10 ev, the mean deflection angle is about 90° and the hard-collision cross section corresponds to the total cross section. At higher electron energies, however, the average momentum exchange corresponds to smaller deflection angles. The total-collision cross section must be reduced by an appropriate amount to obtain the hard-collision cross section.

The hard-collision cross section thus obtained for mercury was also presented in reference 7 and, as discussed in the preceding section of the appendix, was used in the heating-rate calculation. The hard-collision cross section, reduced by the ratio of electron-to-ion mass, was also used to calculate the energy transfer from electrons to ions and neutrals. Experimental data for ions are not available, so the ion hard-collision cross section was assumed to be the same as that for an atom with the same electron energy. The energy loss rate due to hard collisions is, then,

$$\frac{dE}{dt} = \sigma_h \frac{m_-}{m_+} (n_+ + n_o \bar{v}(q_- \bar{V}_-)$$

Excitation and Ionization

The excitation and ionization cross sections were originally obtained from references 13 to 15, although the fairings used were also presented in reference 7. The ionization cross section was used for electron addition to the beam above the ionization energy. The rate of electron addition per cubic centimeter for this process is

$$\frac{dn_-}{dt} = \sigma_i n_- n_o \bar{v}_-$$

The characteristic time is

$$\tau = \frac{n_-}{(dn_-/dt)}$$

For energy loss calculations, the ionization energy of 10.4 ev was used. The excitation energy is somewhat in doubt, but was faired from 4.9 ev at an electron energy of 5 ev to about 7 ev at an electron energy of 100 ev. The energy losses due to collisions with ions were assumed to be the same as those with atoms, although the ion-to-neutral-density ratio was so small that the possible error was unimportant. The energy loss due to exciting and ionizing collisions is, then,

$$\frac{dE}{dt} = [\sigma_e(qV)_e + \sigma_i(qV)_i](n_+ + n_o)\bar{v}_-$$

with $(qV)_e$ and $(qV)_i$ the excitation and ionization energies in ev.

REFERENCES

1. Stuhlinger, E.: Possibilities of Electrical Space Ship Propulsion. Extract from Proc. Fifth Int. Astro. Cong., 1954, pp. 109-119.

2. Sellen, J. M., and Shelton, H.: Transient and Steady State Behavior in Cesium Ion Beams. Preprint 1379-60, Am. Rocket Soc., Inc., 1960.

3. Kaufman, Harold R., and Reader, Paul D.: Experimental Performance of Ion Rockets Employing Electron Bombardment Ion Source. Preprint 1374-60, Am. Rocket Soc., Inc., 1960.

4. Etter, J. E., Eilenberg, S. L., Currie, M. R., and Brewer, G. R.: A New Mechanism of Neutralization of Dense Ion Beams. Paper 1380-60, Am. Rocket Soc., Inc., 1960.

5. Baldwin, George C.: Neutralization of Ion Beams for Propulsion by Electron Trap Formation. Paper 1378-60, Am. Rocket Soc., Inc., 1960.

6. Keller, Thomas A.: NASA Electric Rocket Test Facilities. Paper R-25, Nat. Vacuum Symposium, 1960.

7. Kaufman, Harold R.: An Ion Rocket with an Electron-Bombardment Ion Source. NASA TN D-585, 1961.

8. Francis, Gordon: Ionization Phenomena in Gases, Academic Press, Inc., 1960.

9. Fried, Burton D., and Gould, Roy W.: On the Detection of Ion Oscillations in a Mercury Discharge. Rep. TR-60-0000-GR413, Space Technology Labs., Dec. 9, 1960.

10. Buneman, O.: Dissipation of Currents in Ionized Media. Phys. Rev., vol. 115, no. 3, Aug. 1, 1959, pp. 503-517.

11. Massey, H. S. W., and Burhop, E. H. S.: Electronic and Ionic Impact Phenomena. Clarendon Press (Oxford), 1956.

12. Spitzer, Lyman, Jr.: Physics of Fully Ionized Gases. Interscience Pub., Inc., 1956.

13. Brode, Robert B.: The Quantitative Study of the Collisions of Electrons with Atoms. Rev. Modern Phys., vol. 5, no. 4, Oct. 1933, pp. 257-279.

14. Brown, Sandborn Conner: Basic Data of Plasma Physics. Technology Press, M.I.T., 1959.

15. Harrison, Harry: The Experimental Determination of Ionization Cross Sections of Gases under Electron Impact. Catholic Univ. of Am. Press, 1956.

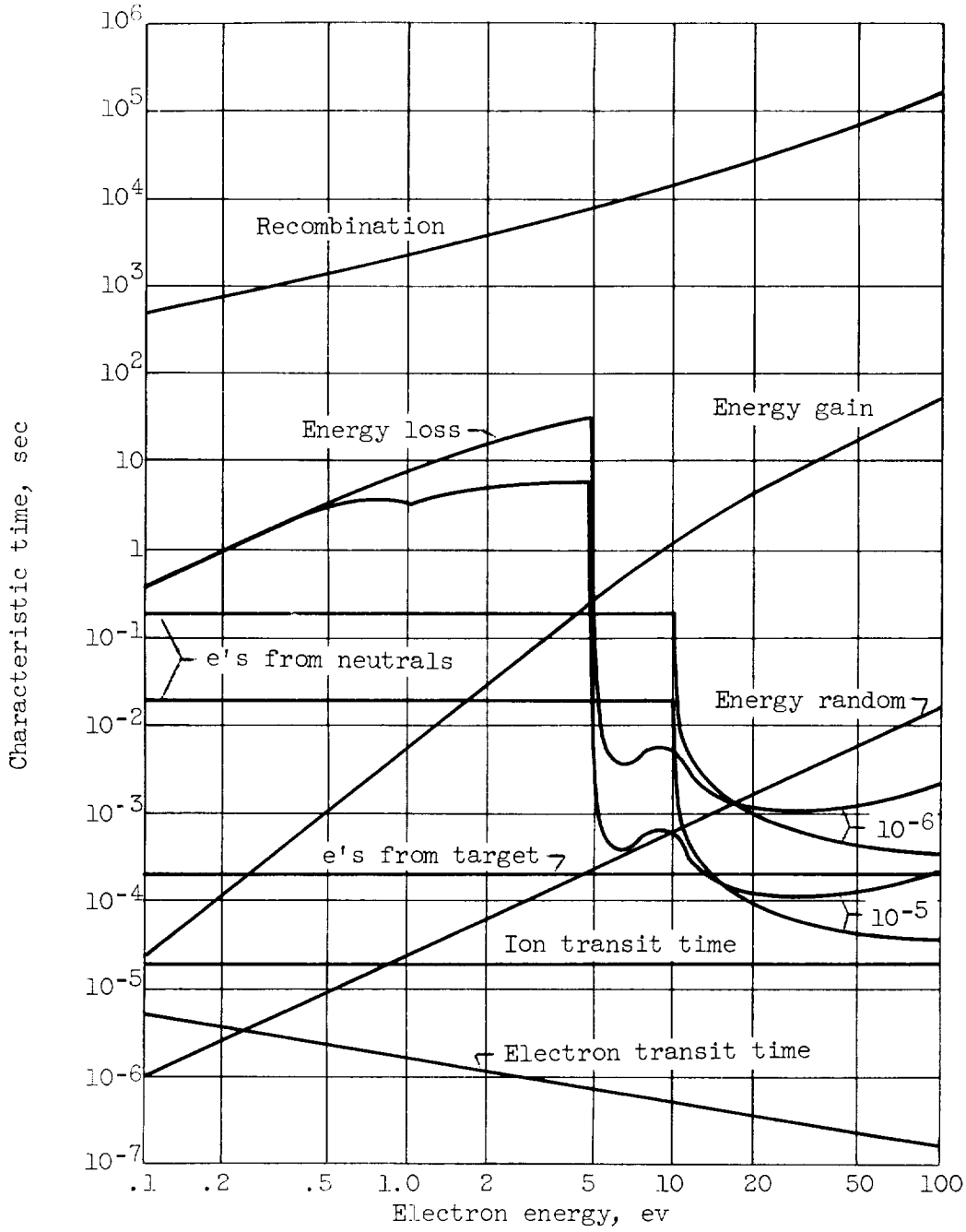

Figure 1. - Characteristic times for collision processes in an ion-rocket beam. Mercury ions were assumed at a density of 10^9 per cm^3, moving at a velocity of 4.9×10^6 cm per second (corresponding to a specific impulse of 5000 sec), over a beam length of 1 meter. Neutrals were assumed to be mercury atoms at a density of 10^{10} per cm^3 for an ion-gage reading of 10^{-6} mm Hg, and 10^{11} per cm^3 for 10^{-5} mm Hg.

NASA - Langley Field, Va. E-1328